Sum-Frequency Vibrational Spectroscopy on Water Interfaces: Polar Orientation of Water Molecules at Interfaces

Yuen Ron Shen* and Victor Ostroverkhov†

Department of Physics, University of California, Berkeley, California 94720

Received May 11, 2005

Contents

1. Introduction 1140
2. Surface Sum-Frequency Vibrational Spectroscopy 1141
3. Sum-Frequency Vibrational Spectra of Water Interfaces 1142
   3.1. Vapor/Water Interfaces 1142
   3.2. Hydrophilic Solid/Water Interfaces 1145
   3.3. Hydrophobic Interfaces 1146
4. Phase-Sensitive Sum-Frequency Vibrational Spectroscopy 1148
5. Phase-Sensitive Sum-Frequency Vibrational Spectroscopy on Quartz/Water Interfaces 1149
6. Discussion 1151
7. Conclusion 1152
8. Acknowledgment 1153
9. References 1153

1. Introduction

Although the importance of water interfaces has long been well recognized, studies of the interfaces at the molecular level only began more recently.[1−3] The difficulty lies in the fact that only a few surface techniques are effective to probe liquid interfaces at the molecular level. Among them, scanning tunneling microscopy (STM) and atomic force microscopy (AFM) may apply to thin films of liquids on solid substrates but suffer from molecular movement at liquid interfaces in the general cases.[4−7] X-ray spectroscopy and neutron reflectivity are more effective and informative,[8−17] but they are not highly surface-specific because they probe a surface layer of ≥ 1 nm and are not easily applicable to buried liquid interfaces. The attenuated total reflection (ATR) method has been used to probe buried liquid interfaces, but it is not very surface-specific, because the wave has a penetration length of ≥ 100 nm into liquid. Recently, optical second-harmonic generation (SHG) and sum-frequency generation (SFG) have become the preferred techniques to study liquid interfaces.[18−22] Being second-order nonlinear optical processes, they are forbidden under electric-dipole approximation in media with inversion symmetry like liquids but necessarily allowed at surfaces or interfaces. They therefore can be highly surface-specific. Furthermore, they can have submonolayer sensitivity and, with the output highly directional, can be used for in situ remote sensing of any interface accessible by light. Over the past 18 years, they have been repeatedly proven to be the most powerful and versatile methods for interrogating surfaces and interfaces. In particular, infrared−visible SFG provides the only means to obtain surface vibrational spectra of liquid interfaces that yield direct information about liquid interfacial structure. One of the very early surface vibrational spectra ever recorded was on a water interface.[23−25]

Several research groups have used sum-frequency vibrational spectroscopy (SFVS) to study various types of water interfaces.[20,22,26−29] The results have aroused great interest in recent years. The surface vibrational spectra generally exhibit a set of characteristic features indicating that the water molecules form a hydrogen-bonding network more ordered than the bulk. Although this is more or less expected from the known surface tension of water, SFVS gives the first molecular-level evidence to the effect. Despite the similarity of the spectra obtained by different groups, however, detailed interpretation of the spectra often varies and causes a great deal of confusion. The difficulty usually arises because of ambiguity in analyzing the spectra and because of lack of sufficiently accurate theoretical calculation to compare with experiment. More recently, a phase-sensitive SFVS technique has been developed, allowing measurements of both the amplitude and the phase of the SF response.[30] It helps in analysis and interpretation of the spectra and is likely to provide a more stringent test of theory on water interfaces.

Intensive theoretical investigation of water interfaces already started half a century ago (see, for example, refs 31 and 32). With the advent of powerful computers, a large number of articles on molecular dynamics and Monte Carlo calculations of water interfaces have appeared in the literature.[33−52] Many of them provide such microscopic information as the density profiles and orientations of water molecules at interfaces. While the qualitative features of various calculations appear the same, the quantitative details can be different depending on the assumed interaction potential between molecules. Both the density profile and the molecular orientation are not directly assessable by experiment. Some calculations have produced surface vibrational spectra that allow direct comparison with experiment,[36,38,39,45,46,53−55] but the accuracy of the calculations is not yet sufficient for the quantitative comparison needed for extracting a detailed structure of a water interface. A very recent paper on SF spectra of a vapor/water interface calculated using an improved time correlation function approach may have bent the trend.[56,57]

This paper reviews the experimental findings by sum-frequency vibrational spectroscopy (SFVS) on water interfaces. It is organized as follows. Section 2 briefly describes the theory and experimental arrangement of SFVS. Section 3 presents the SF vibrational spectra of various water interfaces and discusses the results obtained by various

* Corresponding author. E-mail: yrshen@calmail.berkeley.edu.
† Present address: General Electric Global Research, Niskayuna, NY 12309.

10.1021/cr040377d CCC: $59.00
Published on Web 03/25/2006

Y. Ron Shen is a Professor of Physics at the University of California at Berkeley. He received his Ph.D. in solid-state physics from Harvard University. He is the author of the well-received book *The Principles of Nonlinear Optics* and more than 500 publications in fields ranging from nonlinear optics to laser spectroscopy, surface science, chemical physics, and condensed matter physics. He and his group have developed optical second-harmonic and sum-frequency generation as surface-specific probes for studies of surfaces and interfaces.

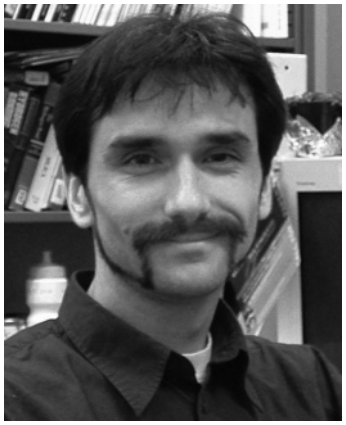

Victor Ostroverkhov was born in Ukraine in 1973. After receiving his undergraduate Diploma in Physics and Optical Engineering from Kiev National Shevchenko University (Kiev, Ukraine) in 1996, he proceeded to do his graduate studies at the Department of Physics, Case Western Reserve University (Cleveland, OH), where he worked in the group of Prof. K. D. Singer on developing novel nonlinear optical techniques and exploring NLO properties of organic materials, and obtained a Ph.D. in Physics in 2001. After graduation, Dr. Ostroverkhov joined the group of Prof. Y. R. Shen at the Department of Physics, University of California, Berkeley, as a postdoctoral researcher. The main focus of his recent work is investigation of aqueous interfaces by means of sum-frequency vibrational spectroscopy (SFVS) and development of the phase-sensitive SFVS technique.

research groups. Section 4 introduces a new SFVS technique that permits simultaneous measurements of amplitude and phase of the SF vibrational spectra for water interfaces. Section 5 then shows how the new technique can yield new information with unprecedented details on the water/silica interfaces. Finally, section 6 summarizes the common features of SF vibrational spectra of water interfaces, discusses usual difficulties in interpretation of spectra, and gives a plausible picture of the water interfacial structure that we conceive from the result obtained with the new SFVS technique.

2. Surface Sum-Frequency Vibrational Spectroscopy

Figure 1 describes a surface SFG process in which two input laser beams at frequencies ω_{vis} and ω_{IR} overlap on a

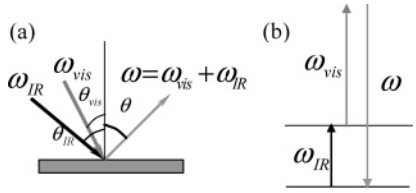

Figure 1. Schematic representation of (a) the sum frequency generation process at an interface detected in the reflection direction and (b) the sum-frequency generation process with ω_{IR} at resonance with a vibrational transition.

sample surface and generate an output at frequency $\omega = \omega_{vis} + \omega_{IR}$ in reflection. It can be shown that the output signal, in photons per second, is given by[19]

$$S(\omega) = \frac{8\pi^3\omega^2 \sec^2\theta}{\hbar c^3 n n_{vis} n_{IR}} |[\vec{\vec{L}}(\omega)\cdot\hat{e}(\omega)]\cdot\vec{\vec{\chi}}_S^{(2)}: [\hat{e}(\omega_{vis})\cdot\vec{\vec{L}}(\omega_{vis})][\hat{e}(\omega_{IR})\cdot\vec{\vec{L}}(\omega_{IR})]|^2 I_{vis} I_{IR} A T \quad (1)$$

where θ is the SF exit angle, $\vec{\vec{L}}(\omega_i)$, $\hat{e}(\omega_i)$, n_i, and I_i are the transmission Fresnel factor, polarization unit vector, refractive index, and intensity of the beam at ω_i, respectively, A is the overlapping beam cross-section on the sample, and T is the input pulse width. We assume here that the SF nonlinear response is dominated by the surface nonlinear susceptibility, $\vec{\vec{\chi}}_S^{(2)}$ of the sample. With ω_{IR} near vibrational resonances (Figure 1b), $\vec{\vec{\chi}}_S^{(2)}$ can be expressed in the form[18,19]

$$\vec{\vec{\chi}}_S^{(2)} = \vec{\vec{\chi}}_{NR}^{(2)} + \sum_q \frac{\vec{\vec{A}}_q}{\omega_{IR} - \omega_q + i\Gamma_q} \quad (2)$$

or if a Gaussian inhomogeneous broadening is assumed for each resonance,[58]

$$\vec{\vec{\chi}}_S^{(2)} = \vec{\vec{\chi}}_{NR}^{(2)} + \sum_q \int d\omega_q \frac{\vec{\vec{A}}_q}{\omega_{IR} - \omega_q + i\Gamma_q} \times \exp\left[-\frac{(\omega_q - \omega_{q_0})^2}{\Delta_q^2}\right] \quad (3)$$

Here, $\vec{\vec{\chi}}_{NR}^{(2)}$ is from the nonresonant contribution, $\vec{\vec{A}}_q$, ω_q, and Γ_q are the strength, resonant frequency, and damping coefficient of the qth vibrational mode, respectively, and ω_{q_0} is the central frequency of the Gaussian profile of the qth mode. When eq 3 is used, Γ_q is usually assumed to be much smaller than Δ_q. In eqs 2 and 3, if interactions between molecules are neglected, $\vec{\vec{A}}_q$ takes the form[18,19]

$$\vec{\vec{A}}_q = N\langle\vec{\vec{a}}_q\rangle \quad (4)$$

where N is the surface density of molecules in the surface layer, $\vec{\vec{a}}_q$ is the tensorial mode strength of individual molecules, and the angular brackets refer to an orientational average over the molecules in the surface layer. As a third-rank tensor describing electric-dipole response, $\vec{\vec{A}}_q$ is nonvanishing only if there exists a net polar orientation of molecules. If the orientational distribution is random, then $\vec{\vec{A}}_q$ vanishes.

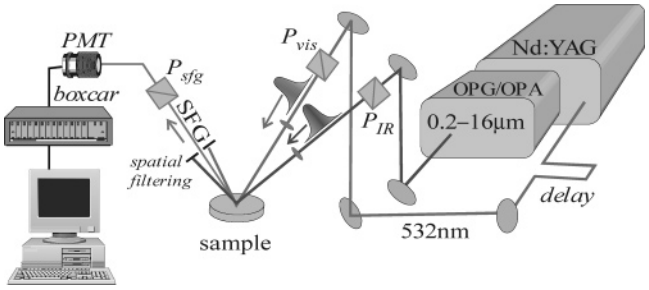

Figure 2. A typical experimental arrangement for SFVS. OPG/OPA refers to an optical parametric generator/amplifier system, and PMT denotes a photomultiplier tube. P_{vis}, P_{IR}, and P_{sfg} are polarizers for visible, IR, and sum-frequency beams, respectively. The propagation direction of the output SF beam is defined by the tangential wave vector matching condition at the interface: $k^{\parallel} = k_{vis}^{\parallel} + k_{IR}^{\parallel}$.

Measurements of the SF output with selected input/output polarization combinations allow determination of various independent elements of $|\vec{\vec{\chi}}_S^{(2)}|$. As ω_{IR} scans over the surface vibrational resonances, the SF output is resonantly enhanced, thus yielding SF surface vibrational spectra. Fitting the spectra with eqs 1 and 2 (or 3) permits deduction of the parameters $\vec{\vec{\chi}}_{NR}^{(2)}$, $\vec{A}_q$, ω_q, and Γ_q or Δ_q for each vibrational mode, providing structural information about the surface or interface. In more complex cases where clear decomposition of a spectrum into individual resonant modes is not possible or reliable, one would have to rely on fitting the observed spectrum by, for example, molecular dynamic calculation to deduce information on the surface structure. This is analogous to determination of the band structure of a crystal from observed spectra of the dielectric constant.

For SFVS on water interfaces, a typical experimental arrangement is shown in Figure 2.[18,19] A picosecond pulsed YAG laser is used to pump an optical parametric generator/amplifier (OPG/OPA) system and produce coherent tunable infrared radiation that covers the frequency range of interest. The infrared pulse and the frequency-doubled pulse from the laser then overlap on the sample to generate SF output in the reflected direction. The output signal was detected and recorded by a photomultiplier and gated integrator system. For details, we refer the readers to ref 19.

The water samples in our experiments were prepared in the usual way. Distilled water with a resistance larger than 18 MΩ·cm and total carbon content less than 10 ppb was used. The vapor/water interface of water in a sealed cell was accessed by light through entrance and exit windows on the cell. The cell was thoroughly cleaned in strongly oxidizing solution before being filled with water. For substrate/water interfaces, access by light was often through the substrate. Before immersion in water, the solid substrates were cleaned in hot chromic acid for several hours and then extensively rinsed with purified water.

3. Sum-Frequency Vibrational Spectra of Water Interfaces

3.1. Vapor/Water Interfaces

SFVS is so far the only method that can produce vibrational spectra for liquid interfaces. Du et al. obtained the first set of vibrational spectra for water interfaces in 1993−1994.[23−25] Figure 3 displays their SSP spectra of the vapor/water interface at various temperatures in comparison with the IR spectra of bulk ice[59] and liquid water.[60] Here,

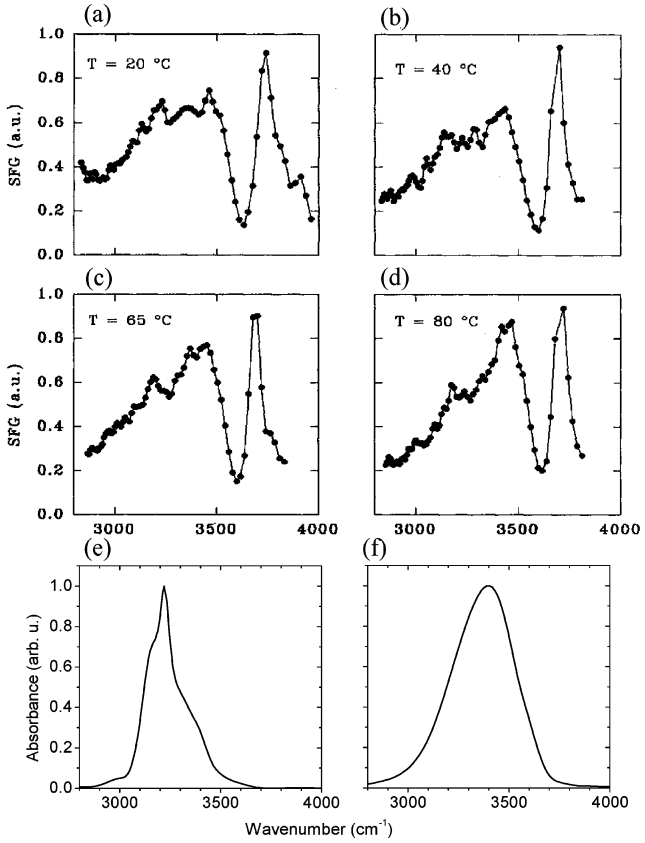

Figure 3. SFVS spectra (a−d) of the water/vapor interface at four temperatures collected with SSP polarization combination (Reprinted Figure 3 with permission from ref 23. Copyright 1993 by the American Physical Society. http://link.aps.org/abstract/PRL/v70/p2313), (e) Bulk absorbance of hexagonal ice (I_h) at 100 K (from data in Bertie et al., ref 59), and (f) bulk absorbance of bulk water (from data in Querry et al., ref 60).

SSP denotes the polarization combination with the SF output, visible input, and infrared input being S-, S-, and P-polarized, respectively. (According to eq 1, the SF signal is proportional to $|\hat{S}\cdot\vec{\vec{\chi}}_S^{(2)}:\hat{S}\hat{P}|^2$; P and S refer to the in- and out-of-plane polarization components with respect to the beam incidence plane.) Although the spectral data exhibit a fair amount of fluctuation, it is clear that the spectra roughly consist of three main peaks. A sharp peak at 3700 cm^{-1} is associated with the stretch mode of the OH dangling bonds at the water surface. Being characteristic of the surface, it is absent in the IR bulk spectra. The two broad peaks at ∼3400 and ∼3200 cm^{-1} are close in positions with the stretch modes of the bonded OH in bulk ice and water. We label them as icelike and liquidlike peaks, respectively. As the temperature increases, the liquidlike peak increases in strength and the icelike peak decreases. These spectra indicate that the water surface structure is partially ordered and partially disordered, presumably in the form of a mixed ordered and disordered hydrogen-bonding network. The temperature dependence of the spectra suggests that the surface structure becomes more disordered at higher temperature, as expected.

In a separate experiment, it was found that the dangling OH peak gradually reduced in strength as methanol was mixed into the bulk water and completely disappeared as the methanol concentration reached 11 vol %.[24] It was known in an earlier surface tension measurement on water/methanol mixtures that at 11 vol % concentration of methanol, the corresponding surface concentration of methanol should be

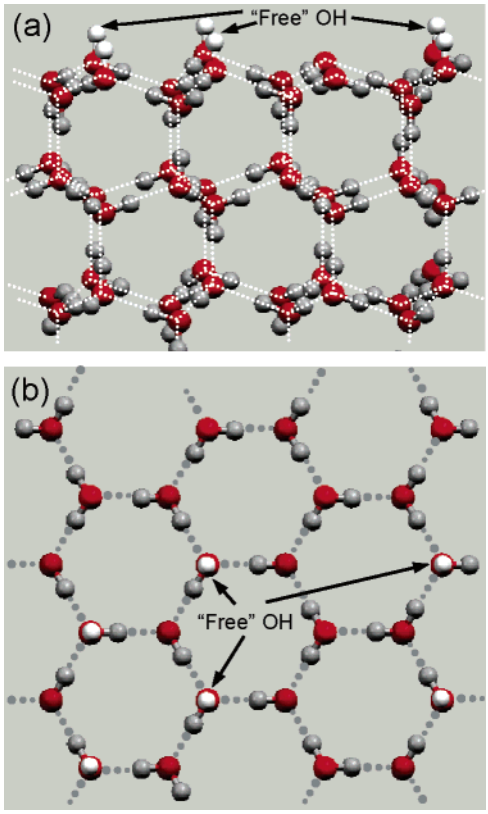

Figure 4. Molecular structure of hexagonal ice (I_h) crystal: (a) side view of the bulk near the (0001) surface; (b) top view of the (0001) plane. Red spheres represent O atoms (dark and light shades highlight higher and lower submonolayers in a single ice monolayer); gray and white spheres represent H atoms that are hydrogen-bonded to neighboring molecules and free-dangling nonbonded surface species, respectively. Dotted lines indicate hydrogen bonds.

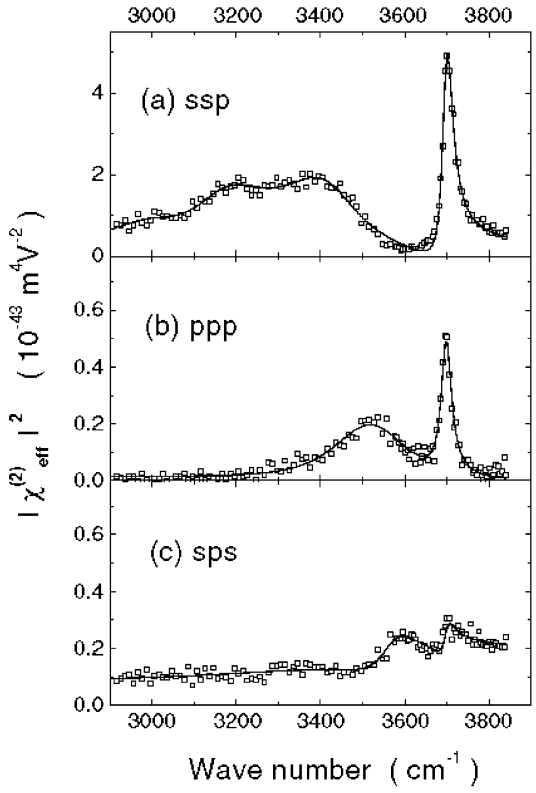

Figure 5. SFG vibrational spectra of water/vapor interface taken with (a) SSP, (b) PPP, and (c) SPS polarization combinations. Reprinted Figure 2 with permission from ref 62. Copyright 2001 by the American Physical Society. http://link.aps.org/abstract/PRL/v86/p4799.

25%.[61] One could then imagine that each methanol molecule at the water surface would have grabbed a dangling OH bond and eliminated its contribution to the dangling OH peak. Complete suppression of the dangling OH peak by ~25% surface concentration of methanol means that there is a quarter monolayer (ML) of dangling OH bonds at a free water surface. This suggests that the water molecules at the surface form a more or less icelike hydrogen-bonding network, although the network is expected to be highly distorted or disordered. As seen in Figure 4, the hexagonal ice has a tetrahedral bonding structure. Each monolayer consists of two submonolayers. At the free ice(0001) surface, each water molecule in the top submonolayer should have one of its tetrahedral bonds broken, and the probability of the broken bonds terminated by H is 50%. This points to the existence of 0.25 ML of dangling bonds in the surface monolayer. These dangling bonds are along the surface normal. Therefore even if the network is severely distorted, their number is not likely to change significantly. We can then conclude that the water surface has a partially disordered icelike structure. This result is also what one would expect from the least number of broken hydrogen bonds at the surface.[35]

Figure 5 shows the improved SF vibrational spectra for a vapor/water interface with three different polarization combinations, SSP, PPP, and SPS, obtained more recently by Wei.[62] All the peaks in the SPS and PPP spectra are significantly weaker than those in SSP except that the SPS spectrum appears to have an extra peak at 3600 cm^{-1}. This is usually an indication that the surface molecules are fairly well oriented, thus again supporting the notion that the water surface structure is fairly well ordered. The 3600 cm^{-1} peak can be assigned mainly to the bonded OH stretch mode of surface water molecules with one bonded OH and one dangling OH.[62] Because the bonded OH is tilted close to the surface plane, its stretch mode is more easily excited by S-polarized, rather than P-polarized, IR input. To confirm the assignment, a polar orientation measurement must show that the bonded OH is pointing away from the interface.

Several other laboratories have also conducted SFVS on vapor/water interface.[22,27,63−80] The observed spectra are nearly the same. Richmond and co-workers found a small peak, not seen by others, at the blue tail of the dangling OH peak in their SSP spectrum.[66,81,82] They used eq 3 in eq 1 to fit the spectrum and obtained two additional vibrational resonance modes at 3662 and 3763 cm^{-1} overlapping with the dangling OH mode at 3700 cm^{-1},[66] which they assign to surface molecules with both OH not bonded to neighbors (labeled as vapor phase molecules). Their interpretation was supported by molecular dynamics simulations[49,50] and by X-ray spectroscopic measurement of Saykally and co-workers.[12,83] This result is rather surprising because the surface density of such molecules, if indeed present, would be very small and their detection by SFVS would be very difficult. In a more recent article, however, Raymond and Richmond stated that these peaks do not exist at a neat water/vapor interface.[68,69] The confusion seemed to come from analyses of the measured spectra. As we shall discuss in a later section, fitting a sum-frequency vibrational spectrum of $|\vec{\chi}^{(2)}_S|$ with eq 2 or 3 in eq 1 is somewhat arbitrary

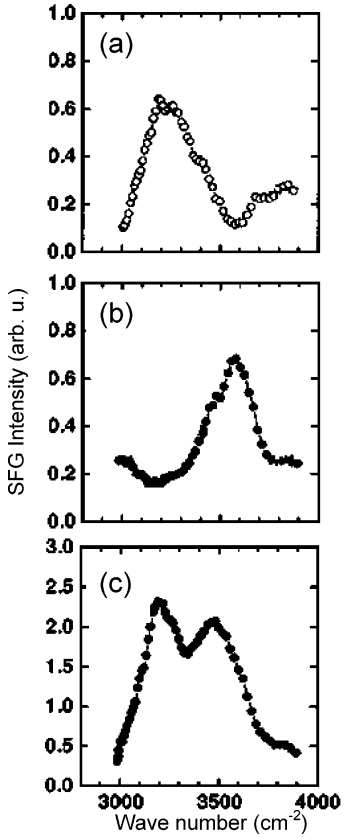

Figure 6. SFG spectra of water interfaces with (a) an octadecanol monolayer on water and (b,c) a hexacosanoic acid monolayer on water at (b) pH = 3.9 and (c) pH = 8.0. Reprinted from ref 84, Copyright 1998, with permission from Elsevier.

without knowledge of the phase of $\vec{\vec{\chi}}_S^{(2)}(\omega)$ or signs of $\vec{\vec{A}}_q$ for different modes. Much of the uncertainty in interpreting the SF vibrational spectra would be removed if the latter could be measured. (In a recent theoretical paper, Space and co-workers[57] suggested that the wagging mode of a similar species at ~875 cm^{-1} may be observable but not the stretch mode.)

A monolayer of molecules covering the free water surface can significantly change the surface water structure. As seen in Figure 6a,b, the spectrum of a long-chain-alcohol-covered water interface has a much more prominent icelike peak,[20,23] while that of a fatty-acid-covered water surface is very much distorted from the free water spectrum.[20,84] The former suggests a more polar-ordered hydrogen-bonding water network and the latter a more distorted one assuming that there is no surface field. In a classical experiment, Leiserowitz et al. demonstrated that the freezing temperature of a water drop could increase by several degrees if it was coated by a monolayer of long-chain alcohol.[85] They found that the lattice of the alcohol monolayer matches fairly well with that of the hexagonal face of ice and could help induce ice nucleation in neighboring water through epitaxial interaction. We can expect that the same mechanism would induce a more ordered icelike structure in the water interfacial layer, as the spectrum seemed to have shown. On the other hand, the fatty acid monolayer has a significant lattice mismatch with ice. The interaction between water and fatty acid molecules would significantly distort the usual icelike hydrogen-bonding network of the surface water layer. Ionizing the fatty acid monolayer by increasing pH in bulk water, however, produces a surface field that can orient and restore the more ordered icelike surface water structure.[84] This was actually reflected in the SF spectrum displayed in Figure 6c. Richmond's group has studied in detail the effects of temperature, ionic strength, and surface charge density on the spectrum and structure of the interfacial water layer beneath charged surfactant layers.[63−65] They observed that the water layer approached its best polar ordering (in terms of the strength of the icelike peak) long before the surface charge reached its maximum. Patey and Torrie predicted earlier that a surface field could induce more ordering in the hydrogen-bonding network of an interfacial water layer.[86]

Earlier SFVS measurement by Du et al. found no appreciable change in the vibrational spectrum of a vapor/water interface upon dissolution of up to 0.5 M NaCl.[23,24] Raduge et al. studied water−sulfuric acid mixtures.[87] They observed that as the concentration of sulfuric acid first increased, the surface water spectrum appeared stronger in the icelike region, presumably because of more polar ordering of the surface water network. At very high sulfuric acid concentrations, the spectrum became weaker and finally disappeared. It was believed that the sulfuric acid molecules at such high concentrations are no longer ionized and they form a quasi 2-D crystalline structure at the surface that would not contribute to the SFG. Schultz and co-workers obtained similar results and suggested that the spectral enhancement was due to surface-field-induced ordering of water molecules in a double-charge layer formed by cations and anions at the surface.[70,72,73,88] They however believed that the decrease of the spectral intensity at high sulfuric concentrations were due to disruption of the water hydrogen-bonding network by ion complexes or sulfuric acid molecules at the surface.[73] They have also studied the effects of other acids and salts on the water surface, and concluded that ions appearing at the surface could influence the surface water spectrum via surface-field-induced reorientation of surface water molecules.[74−76,89] More recently, additional investigations, both theoretical and experimental, have confirmed that sufficiently high concentration of acid, base, and salt could affect the vapor/water interfacial structure.[26,27,37,40−42,52,69,80,90] Molecular dynamics simulations predict that larger and more polarizable negative ions would have more excess at the water surface, while positive ions would be repelled from the surface.[37,40−42] The SFVS result of Liu et al. on aqueous sodium halide solutions supported the conclusion,[27,80] and so did the recent SHG result of Saykally and co-workers.[91−93] (No appreciable change of the spectrum was observed with dissolution of NaCl up to 1.5 M, consistent with the earlier result of Du et al.[23,24]) Richmond's group also reported an SFVS study on solutions of halides in mixtures of normal and heavy water.[69] They found that the icelike (tetrahedral bonding) peak seemed to be most sensitive to change of the anion from F^- to I^-, and two new peaks at ~3650 and ~3750 cm^{-1} appeared that could be assigned to weakly bonded water molecules solvating the ions. They then concluded that the anions would not approach the topmost water layer but rather spread throughout a wider interfacial region, perturbing (in the case of Cl^-, Br^-, and I^-) or enhancing (F^-) the hydrogen-bond network. This conclusion is in conflict with the molecular dynamics predictions by Jungwirth and Tobias,[40−42] as well as the recent X-ray photoelectron spectroscopy studies by Salmeron and co-workers.[8]

With acid in water, hydronium ions likely appear at the surface with their oxygen end facing the surface.[80,94,95] Figure 7 presents the interfacial water spectra of different solutions

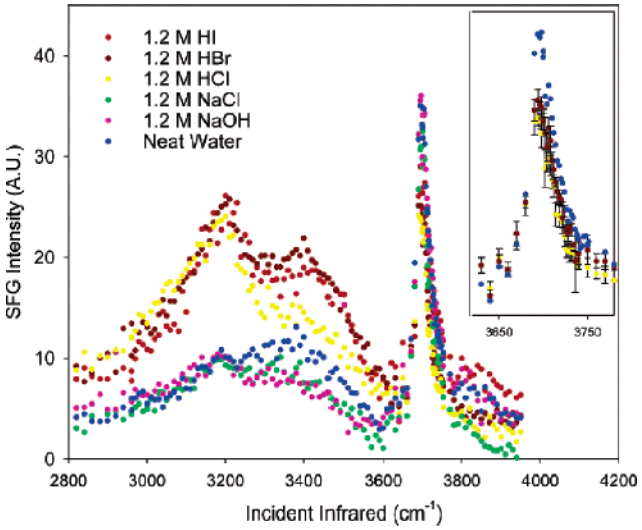

Figure 7. SFG spectra of water/vapor interfaces for neat water and several acid, base, and salt solutions. The inset shows an extended view of the dangling OH peak on neat water (blue), 1.2 M HCl (yellow), and 1.2 M HBr (brown). Reprinted with permission from ref 80. Copyright 2005 American Chemical Society.

reported by Allen and co-workers.[80] Compared with the spectrum of the neat water, the icelike peak for acid solutions appears significantly stronger. It was interpreted as due to the presence of hydronium ions at the surface, although their vibrational resonances and polar orientation are yet to be identified. For solutions of HBr and HI, both icelike and liquidlike peaks show significant enhancement, which can be understood as due to the presence of a surface field created by excess negative ions at the surface. The free-OH peaks for the acidic solutions are weaker and were also interpreted as due to hydronium ions at the surface. Obviously, at this point, all interpretations appear somewhat speculative. They could be substantiated or refuted provided that the polar orientations of the OH bonds responsible for the various spectral peaks could be determined.

3.2. Hydrophilic Solid/Water Interfaces

SFVS is also the only vibrational spectroscopic tool for probing buried interfaces, in particular, the solid/liquid interfaces. The first SF vibrational spectra of solid/liquid interfaces are on hydrophilic fused silica/water interfaces obtained by Du et al. at various bulk pH values.[25] The same interfaces were also studied by others using SFVS.[96−99] The spectra obtained by different groups are qualitatively the same, but there were some quantitative differences that could be traced to instability of the surface structure of silica in water undergoing the equilibrium reaction $SiOH \rightleftarrows SiO^- + H^+$.[99] We present in Figure 8b a set of recently measured SSP spectra of silica/water interfaces at different bulk pH.[100] It is seen that they are qualitatively the same as that of the vapor/water interface except that the dangling OH peak at 3700 cm^{-1} is missing. The presence of the liquidlike and icelike peaks indicates that the interfacial water molecules must again form a partially ordered hydrogen-bonded network. Both peaks increase with pH, but the icelike peak grows more appreciably at high pH, suggesting a better polar-ordered network at high pH.

It is known that a fused silica surface properly cleaned in acid and rinsed by water is passivated by hydrogen. When immersed in water, it adjusts to the equilibrium structure

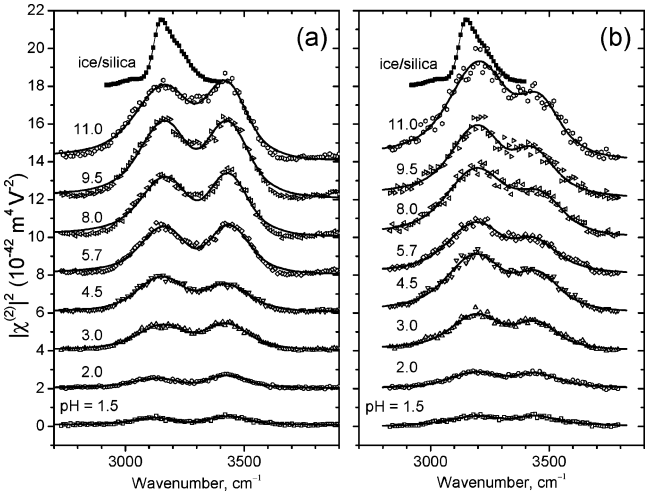

Figure 8. SFG spectra of interfaces of water with (a) the (0001) plane of α-quartz and (b) fused silica as a function of pH. Polarization combination is SSP. A spectrum of the ice/fused silica interface is shown for comparison (filled squares). The spectra are offset vertically by 2 units for clarity. Reprinted from ref 100, Copyright 2004, with permission from Elsevier.

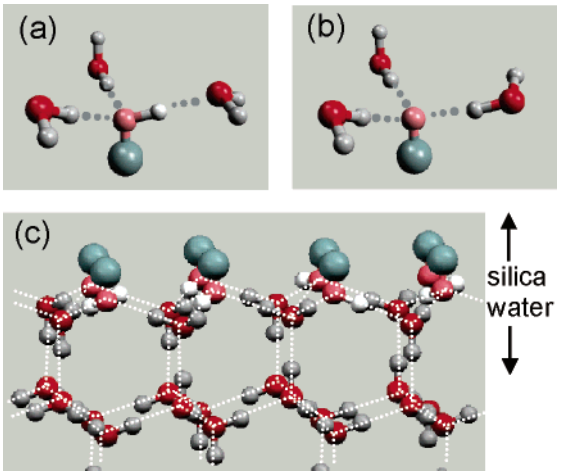

Figure 9. Possible hydrogen-bonding configuration of water molecules on hydrophilic silica surface: (a) protonated (SiOH) surface sites, low pH; (b) deprotonated (SiO^-) surface sites, high pH; (c) structure of water/silica interface at low pH. Red and gray spheres represent O and H atoms of water molecules; large gray-green, pink, and white spheres represent Si, O, and H atoms of SiOH groups at silica surface. Dotted lines indicate hydrogen bonds.

dictated by the reaction $SiOH \rightleftarrows SiO^- + H^+$. According to the literature,[101] the surface remains as SiOH in the neutral state, if the pH of bulk water is lower than 2, becomes increasingly deprotonated as pH increases, and is completely deprotonated and saturated with negative charges at pH ≥ 10 that produce a surface field of $\sim 10^7$ V/m. To both neutral (SiOH) and charged (SiO^-) surfaces, the water molecules can be bonded via hydrogen bonding (see Figure 9). In the former case, two molecules can bind with H to O and one with O to H on SiOH. In the latter case, three molecules can bind with H to O of SiO^-. In both cases, the dangling OH bonds are eliminated. The strong surface field at high pH should help orient the water molecules with H bonding to the surface and establish a more ordered hydrogen-bonding network. This was predicted earlier in molecular dynamics simulation by Lee and Rossky[34,35] and now seems to be confirmed by SFVS.

We note that as a second-order nonlinear response, $\vec{\vec{\chi}}_S^{(2)}$ of SFVS will have its phase changed by 180° if the net polar orientation of interfacial water molecules is reversed, as presumably occurs when the bulk pH switches from low to high value. To prove the phase change, we need an interference measurement on the SF output. This was actually demonstrated by Du et al. at the peak frequency of the icelike peak.[25] However, as we shall see later, icelike and liquidlike peaks come from different interfacial water species. They respond differently to change of pH. Therefore, for a complete picture of how water molecules reorient at the interface in response to pH variation, we need to know how the phase of $\vec{\vec{\chi}}_S^{(2)}(\omega)$ changes over the spectrum. As we mentioned earlier, the experimentally determined phase of $\vec{\vec{\chi}}_S^{(2)}(\omega)$ or the signs of $\vec{A}_q$ are generally important. Without them, a mere fit of a spectrum by eq 1 could lead to incorrect interpretation of the spectrum.

Yeganeh el al. used SFVS to probe alumina/water interfaces and also observed the icelike and liquidlike peaks.[102] They found that the spectrum varied with pH and the overall strength of OH stretch modes reached a minimum at pH $\approx$ 8. Fitting of the spectra suggested that $\vec{\vec{\chi}}_S^{(2)}(\omega)$ was 180° out of phase at high and low pH. Thus pH = 8 appeared to be the isoelectric point for the interface. The alumina surface would be positively and negatively charged below and above pH = 8, respectively, under the reactions $AlOH + H^+ \rightleftarrows AlOH_2^+$ and $AlOH \rightleftarrows AlO^- + H^+$. The surface field resulting from the surface charges would reorient the interfacial water molecules to yield the net polar orientations observed from $\vec{\vec{\chi}}_S^{(2)}(\omega)$. Clearly, their interpretation should be checked or substantiated by measuring the phase of $\vec{\vec{\chi}}_S^{(2)}(\omega)$. Richmond and co-workers studied CaF_2/water interfaces with SFVS and observed again both the icelike and the liquidlike peaks and their dependence on pH.[103,104] Below the isoelectric point, the surface having had F^- dissolve into water became positively charged. The resulting surface field oriented the interfacial water molecules and made the icelike peak significantly stronger than the liquidlike peak. Controlled adsorption of sodium dodecyl sulfate (SDS) surfactant anions on the surface could be used to adjust the net surface charge density.[104,105] As the surface charge density changed from positive to negative, the intensity of the SF vibrational spectrum first decreased, went through a minimum at the zero-charge point, and then increased. Presumably $\vec{\vec{\chi}}_S^{(2)}(\omega)$ had undergone a 180° phase shift upon crossing over the zero-charge point, and the interference between the CH stretch modes of SDS and OH modes of water seemed to have supported the interpretation. However it is unclear whether the orientation of the CH_x groups could be regarded as unchanged in their analysis when the adsorbed SDS formed bilayers.

Cremer and co-workers studied water interfaces with bare silica and silica covered by a thin film of TiO_2 nanoparticles.[106] They observed different pH dependence of the SF spectrum for the two interfaces because of the shift of the point of zero charge. Adsorption of charged polymers on the bare quartz surface also significantly alters the point of zero charge. Adsorption of phosphate buffer ions on TiO_2 enhanced the liquidlike peak relative to the icelike peak. They interpreted the result as due to blocking of surface registry sites by phosphate ions and forcing the interfacial water molecules to form a more disordered hydrogen-bonding network. This interpretation does not take into consideration possible change of polar orientation of water molecules. Again, its validity can be tested by the phase measurement of $\vec{\vec{\chi}}_S^{(2)}(\omega)$.

Nihonyanagi et al. applied SFVS to a gold/electrolyte interface with an external potential.[29] With the potential varied across the zero-charge point, the liquidlike peak reduced to a minimum and increased again, suggesting maximum molecular disordering when the surface was neutral. From the interference of the water spectrum with the background contribution from the gold substrate, the authors concluded, however, that water molecules remained oriented with their hydrogens toward the surface even after the surface potential had switched from negative to positive. They suspected that it was the result of the sulfate ion adsorption onto the surface at positive potentials, but this explanation seemed to be in conflict with the observed change of the liquidlike peak.

Ostroverkhov et al. obtained SF vibrational spectra of water/α-quartz(0001) interfaces for different pH values and compared them with those of the water/silica interfaces in Figure 8.[100] The two sets are qualitatively very similar, but the icelike peak of the former is red-shifted by $\sim$50 cm^{-1}, much closer in position to the real ice peak (also shown in Figure 8 for comparison). The frequency shift suggests that the water structure next to α-quartz is more ordered. In fact, there exists in the literature a conjecture that the interfacial water structure next to a crystalline face should be more ordered, presumably because of quasi-epitaxial lattice matching. Here, the SFVS result seems to have provided the first evidence. We note that the water/crystalline alumina spectrum of Yeganeh et al. also revealed an icelike peak red-shifted by $\sim$50 cm^{-1}.[102]

It is fair to say that the interfacial water structure next to a hydrophilic solid surface generally appears as a mixed ordered and disordered hydrogen-bonding network, as characterized by the icelike and liquidlike peaks in the vibrational spectrum. (Recent X-ray and electron diffraction studies of several crystal/water interfaces also reported the observation of coexistence of icelike and liquidlike structure at the interfaces.[14,107,108]) The details may vary depending on how the interfacial water molecules bond to the solid surface, which can be affected by modification of the surface through deprotonation, ion adsorption, or molecular adsorption at the surface. Surface charges, and hence surface field, can induce more polar ordering of interfacial water molecules perhaps even up to a few monolayers. However, the direction of polar orientations of interfacial water molecules often cannot be determined from the conventional SFVS with certainty. To obtain information on polar orientation, phase measurement of $\vec{\vec{\chi}}_S^{(2)}(\omega)$ is important.

3.3. Hydrophobic Interfaces

Water molecules wet a hydrophobic surface poorly because they interact less strongly with the substrate than among themselves. Air is an ideal hydrophobic surface; water curls up into a droplet in air. Therefore we would expect the surface vibrational spectrum of water at the interface with a strongly hydrophobic substrate to be similar to that of the vapor/water interface. In particular, the peak from the dangling OH bonds should show up since they would not be bonded to the substrate. This was actually first observed by Du et al. for a water/OTS-covered silica interface.[24]

As mentioned earlier, molecular adsorption on a substrate can drastically alter the surface properties. In the case of a

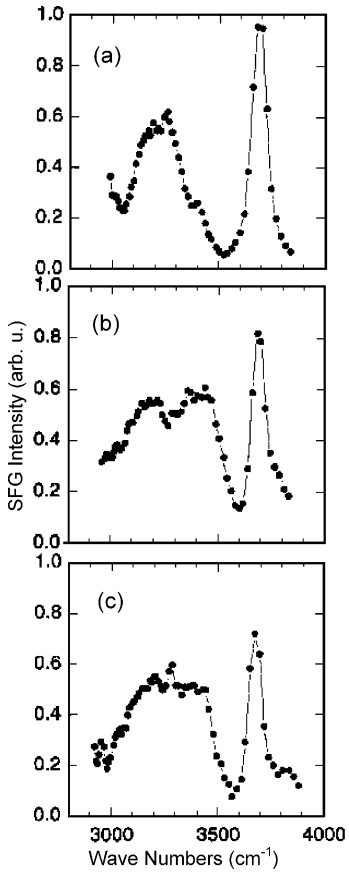

Figure 10. SFG spectra of water on solid and liquid hydrophobic interfaces: (a) water/octadecyltrichlorosilane (OTS)/fused silica interface; (b) water/vapor interface; (c) water/hexane interface. Reprinted with permission from *Science* (http://www.aaas.org), ref 24. Copyright 1994 AAAS.

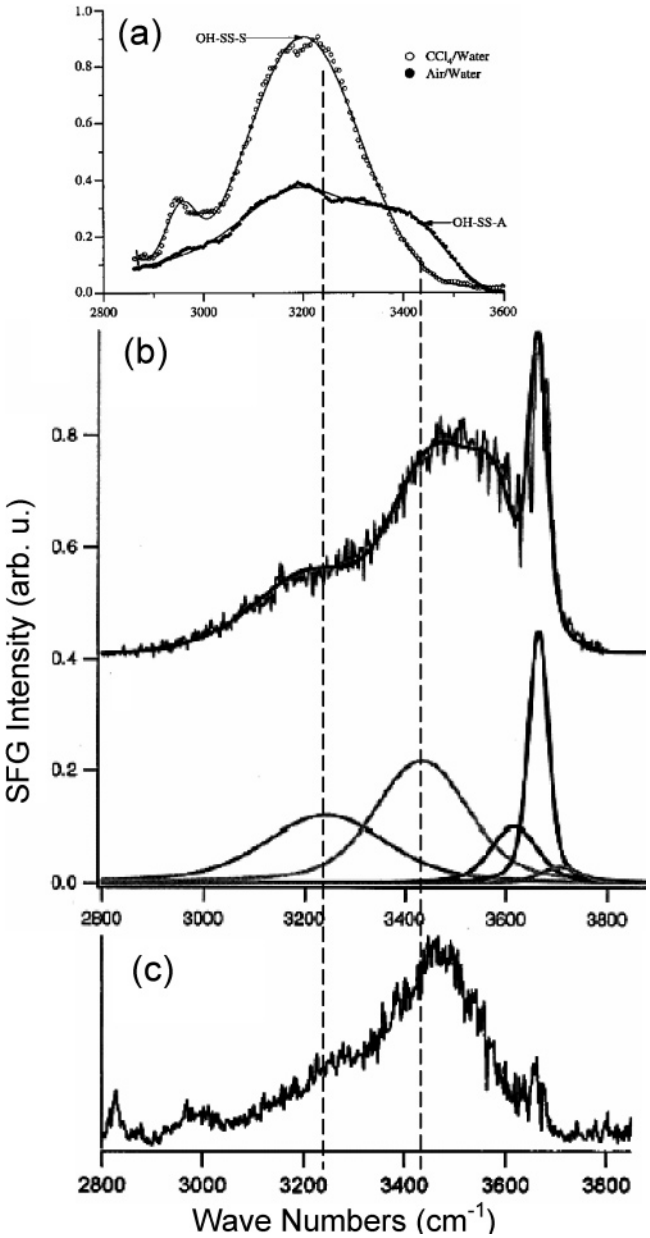

Figure 11. SFG spectra of water−oil interfaces: (a) spectra of water/vapor and water/CCl_4 interfaces from an earlier work (Reprinted with permission from ref 65. Copyright 1998 American Chemical Society); (b) spectrum of water/CCl_4 interface from Brown et al. (Reprinted with permission from ref 66. Copyright 2000 American Chemical Society)—the solid line is a fit using the modes described by the bottom curves; (c) spectrum of water/hexane interface (Reprinted with permission from ref 110. Copyright 2001 American Chemical Society). Vertical lines are guide to the eye for the positions of icelike and liquidlike peaks of decomposition in panel b.

well-prepared surface monolayer of octadecyltrichlorosilane (OTS) on silica, the surface appears as tightly packed hydrocarbon chains with all-trans conformation and is therefore highly hydrophobic. Figure 10 displays the SSP surface vibrational spectrum of a neat water/OTS-covered silica interface in comparison with that of the neat water/vapor interface.[24] The free-OH peak appears at 3680 cm^{-1}, which is red-shifted by ~20 cm^{-1} from that of the water/vapor interface. This indicates that there is no bonding between water and OTS, but there still exists weak van der Waals interaction between the free OH and the CH_3 terminal group of OTS to cause the red shift. The bonded OH spectrum exhibits the characteristic icelike and liquidlike features, but the icelike peak is relatively more prominent. A plausible explanation is that in contrast to the free water surface, the OTS-covered silica surface has a rigid wall that could force the interfacial water molecules to form a more ordered bonding network. One would then argue that if this were true, a water/oil interface that is not rigid would have a spectrum more like that of the water/vapor interface. Indeed, as shown in Figure 10c, the spectrum of a water/hexane interface looks quite similar to that of the water/vapor interface.[24]

Molecular dynamics simulations gave a picture in fair agreement with that presented above.[33,35] They found that the need to maximize the number of hydrogen bonds at the surface and to satisfy the restriction on molecular arrangement imposed by the rigid wall makes water molecules next to a solid hydrophobic surface form a better ordered bonding network. The calculations also showed that water molecules at a water/decane interface have an orientational distribution very similar to that of the water/vapor interface.[33,109]

Richmond's group has investigated extensively water/oil interfaces using SFVS.[65,110−114] In the earlier work by Gragson and Richmond,[65] the spectrum of the neat water/CCl_4 interface showed mainly a broad icelike peak (Figure 11a), which increased in strength when sodium dodecyl sulfate (SDS) surfactant ions increasingly adsorbed at the interface. Scatena et al. later found for the same interface a relatively weak icelike peak and a more prominent liquidlike

peak that was blue-shifted to ~3500 cm^{-1} (Figure 11b).[66,111] They believed that the earlier spectrum suffered from contamination at the interface, because less than 1 μM SDS in water could change the spectrum of Figure 11b to one like that of Figure 11a.[113] Following the earlier work of water/vapor interface,[66,81,82] they identified through fitting of the spectrum five modes contributing to the spectrum. In addition to the icelike, liquidlike, and dangling OH peaks, there were also the symmetric and antisymmetric OH stretch modes of surface water molecules at 3618 and 3708 cm^{-1} that had both of their H ends not bonded to neighbors.[66,111] (We notice that these experiments were all performed with the visible input in and the infrared input around the total internal reflection (TIR) geometry. The Fresnel coefficient for the infrared beam had a rather strong dispersion as the infrared frequency tuned over the vibrational resonances of water. To obtain the correct spectrum of $|\vec{\chi}_S^{(2)}(\omega)|^2$, care must be taken to correct for such a dispersion.) Molecular dynamics simulations seemed to have supported the picture.[43,44,51] However, in more recent articles studying water/vapor interfaces of alkali halide solutions, Richmond and coworkers also found such symmetric and antisymmetric modes and assigned them to water molecules associated with halide ions at the interface.[69,112] Scatena et al. also obtained a similar spectrum for the water/hexane interface, as shown in Figure 11c.[110,111] Compared to the water/hexane spectrum of Figure 10c, their spectrum also appears to be blue-shifted. The spectra of water interfaces with hexane and other alkanes obtained later by Brown et al. showed less of the blue shift and a more pronounced free OH peak.[54] Thus it is not clear what the true spectrum of a neat water/oil interface is. Molecular ions that can be easily segregated to the interface certainly will affect the interfacial water structure, and hence the spectrum, via the surface field. The change could be more clearly recognized from measurement of the complex $\vec{\chi}_S^{(2)}(\omega)$.

Richmond's group did study modification of water/oil interfaces by purposely adsorbing molecular ions, including SDS.[112,113] As expected, the adsorbed ions created a surface field that enhanced the surface water spectrum. Depending on the net charge at the interface, the interfacial molecules would have their net polar orientation with either the oxygen end or the hydrogen end facing the interface. Again, this is a picture that could be confirmed if the polar orientation of interfacial water molecules were measured.

4. Phase-Sensitive Sum-Frequency Vibrational Spectroscopy

In the previous sections, we have repeatedly stressed the importance of measuring both the amplitude and the phase of $\vec{\chi}_S^{(2)}(\omega)$, but the signal $S(\omega)$ from conventional SFVS yields only $|\vec{\chi}_S^{(2)}(\omega)|$ through eq 1. It displays spectral features through resonance enhancement of $|\vec{\chi}_S^{(2)}(\omega)|$. The strength of each mode, $\vec{A}_q$ in $\vec{\chi}_S^{(2)}(\omega)$, is nonvanishing only if the assembly of contributing molecules has a net polar orientation, and its sign depends on the direction of the net polar orientation. Interference of contributions to $\vec{\chi}_S^{(2)}(\omega)$ from resonant modes generally makes the spectrum appear more complex. Fitting a spectrum with eqs 1 and 2 (or 3) can, in principle, determine the relative signs of $\vec{A}_q$. This has been the practice in analyzing and interpreting the spectra of water interfaces in the past. However, because of the limited quality of the spectrum, the signs of $\vec{A}_q$ so obtained

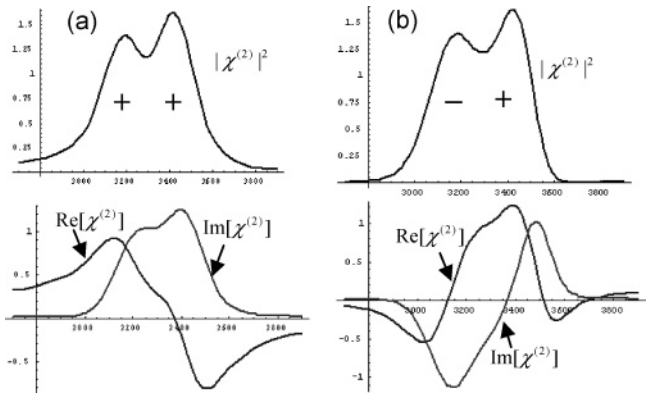

Figure 12. Simulated spectra of two overlapping spectral peaks with amplitudes having (a) the same relative sign and (b) the opposite signs. The $|\chi^{(2)}|^2$ spectra are generated from the corresponding spectra of Re[$\chi^{(2)}$] and Im[$\chi^{(2)}$].

are often not reliable. Figure 12 shows an example relevant to the bonded OH spectra of water: The $|\vec{\chi}_S^{(2)}(\omega)|$ spectra in Figure 12a,b appear hardly distinguishable, although one is composed of two resonance modes with the same sign and the other of opposite signs. One would like to obtain the phase of $\vec{\chi}_S^{(2)}(\omega)$ directly from experiment and thus unambiguously determine the relative signs of $\vec{A}_q$. More generally, one hopes to directly measure $\vec{\chi}_S^{(2)}(\omega)$ (both amplitude and phase) since it carries the complete information on the nonlinear response of the system. As was already known in the early days of nonlinear optics, the phase measurement can be achieved by an interference method,[115] although such measurements over an entire spectrum are extremely rare.[116−118] We have recently done the complete measurement on $\vec{\chi}_S^{(2)}(\omega)$ for water/quartz interfaces.[30] Here, we discuss the essence of our phase-sensitive (PS) SFVS technique.

Consider a water interface with a substrate whose bulk has a nonnegligible contribution to the SF generation. Then, instead of eq 1, the overall SF signal is given by[19]

$$S(\omega) = \frac{8\pi^3\omega^2 \sec^2\theta}{\hbar c^3 n n_{vis} n_{IR}} |[\vec{L}(\omega)\cdot\hat{e}(\omega)]\cdot\vec{\chi}_{eff}^{(2)}: [\hat{e}(\omega_{vis})\cdot\vec{L}(\omega_{vis})][\hat{e}(\omega_{IR})\cdot\vec{L}(\omega_{IR})]|^2 I_{vis} I_{IR} A T$$

$$\vec{\chi}_{eff}^{(2)} = \vec{\chi}_S^{(2)} + \vec{\chi}_B^{(2)}/(i\Delta k) \quad (5)$$

where $\vec{\chi}_B^{(2)}$ is the bulk nonlinear susceptibility of the substrate and $\Delta k = |k_{vis,z} + k_{IR,z} - k_z|$ is the wave-vector mismatch of SFG along the surface normal direction. For a given input/output polarization combination, we have

$$S(\omega) \propto |\chi_S^{(2)} + \chi_B^{(2)}/(i\Delta k)|^2 = |\chi_S^{(2)}|^2 + |\chi_B^{(2)}/\Delta k|^2 - 2|\chi_S^{(2)}\,\chi_B^{(2)}/\Delta k| \sin\Phi(\omega) \quad (6)$$

where $\Phi(\omega)$ is the relative phase of $\chi_S^{(2)}$ with respect to $\chi_B^{(2)}$ or simply the phase of $\chi_S^{(2)}$ if $\chi_B^{(2)}$ is real. Equation 6 shows that if $S(\omega)$, $|\chi_S^{(2)}(\omega)|$, and $|\chi_B^{(2)}(\omega)/\Delta k|$ can be separately measured, then $\Phi(\omega)$ can be determined.

We can imagine finding a substrate with an adjustable $|\chi_B^{(2)}(\omega)/\Delta k|$. With $|\chi_B^{(2)}(\omega)/\Delta k|$ adjusted to zero, we have $S_S(\omega) = C|\chi_S^{(2)}|^2$. With and without water, we have $S_{SB}(\omega) = C|\chi_S^{(2)} + \chi_B^{(2)}/(i\Delta k)|^2$ and $S_B(\omega) = C|\chi_B^{(2)}/\Delta k|^2$, respec-

tively. Here, C is a proportional constant. We then find

$$\Phi(\omega) = \sin^{-1}\left\{-\frac{S_{SB}(\omega) - S_S(\omega) - S_B(\omega)}{2[S_S(\omega)S_B(\omega)]^{1/2}}\right\} \quad (7)$$

In our experiment to be discussed later, we employed a crystalline α-quartz as the substrate that has nonlinearity dominated by $\chi^{(2)}_{B,XXX} = -\chi^{(2)}_{B,XYY} = -\chi^{(2)}_{B,YXY} = -\chi^{(2)}_{B,YYX}$.[119] Since quartz is transparent in the OH stretch region of interest, $\vec{\chi}^{(2)}_B$ can be taken as real, thus simplifying the analysis. We consider here a quartz plate with its c-axis normal to the surface and SFVS with SSP polarization combination. Because of the 3-fold symmetry of quartz about the c-axis, we have $\chi^{(2)}_B(\mathrm{SSP}) = 0$ if the X-axis of the quartz plate is rotated by angle $\phi = 30°$ from the incidence plane. Then if the SF polarization is selected to be off by a small angle $\pm\gamma$ from the S polarization, we have

$$\chi^{(2)}_B(\mathrm{S}_{\pm\gamma}\mathrm{SP}) = \mp\gamma\chi^{(2)}_{B,XXX}\cos\theta_{IR}\cos\theta_{SF} \quad (8)$$

where θ_{IR} and θ_{SF} are the angles between the X-axis and the IR and SF fields at ω_2 and ω, respectively. For the water/quartz interface, the corresponding surface nonlinearity is

$$\chi^{(2)}_S(\mathrm{S}_{\pm\gamma}\mathrm{SP}) = \chi^{(2)}_{S,xxz}\cos\gamma \quad (9)$$

To find $\Phi(\omega)$ from eq 7, $\chi^{(2)}_B(\mathrm{S}_{\pm\gamma}\mathrm{SP})$ and $\chi^{(2)}_S(\mathrm{S}_{\pm\gamma}\mathrm{SP})$ are to be used in eq 6. It is also possible to determine $\Phi(\omega)$ from

$$\Phi(\omega) = \sin^{-1}\left\{\frac{S_{SB}(\omega,\gamma) - S_{SB}(\omega,-\gamma)}{4\sqrt{S_S(\omega)S_B(\gamma)}\cos\gamma}\right\} \quad (10)$$

Note that $S_S(\omega) = S_{SB}(\omega,\gamma{=}0) \propto |\chi^{(2)}_S(\omega)|^2$. Thus we can completely determine $\chi^{(2)}_S(\omega) = |\chi^{(2)}_S(\omega)|\exp[i\Phi(\omega)] = \mathrm{Re}[\chi^{(2)}_S(\omega)] + i\,\mathrm{Im}[\chi^{(2)}_S(\omega)]$.

5. Phase-Sensitive Sum-Frequency Vibrational Spectroscopy on Quartz/Water Interfaces

We have applied PS-SFVS to α-quartz(0001)/water interfaces.[30] The experimental arrangement is sketched in the inset of Figure 13. To avoid beam polarization change due to optical activity of quartz, the visible beam was incident from the water side, while the infrared beam was incident from the quartz side at an angle of 56° such that the optical rotation was less than ~0.2°. The SF output was detected from the water side. For each interface, four spectra were taken: $S_{SB}(\omega,\gamma{=}0)$, $S_{SB}(\omega,\gamma{=}5°)$, $S_{SB}(\omega,\gamma{=}-5°)$, and $S_B(\omega,\gamma{=}\pm5°)$. From the spectra, $|\chi^{(2)}_S(\omega)|$ and $\Phi(\omega)$ were deduced and $\mathrm{Re}[\chi^{(2)}_S(\omega)]$ and $\mathrm{Im}[\chi^{(2)}_S(\omega)]$ were calculated. An example is presented in Figure 13, where $S_{SB}(\omega,\gamma{=}0)$, $S_{SB}(\omega,\gamma{=}5°)$, $S_{SB}(\omega,\gamma{=}-5°)$, and $S_B(\omega,\gamma{=}\pm5°)$ for the quart/water interface with bulk pH of 6.5 are displayed in panel a and $|\chi^{(2)}_S(\omega)|$, $\mathrm{Re}[\chi^{(2)}_S(\omega)]$, and $\mathrm{Im}[\chi^{(2)}_S(\omega)]$ in panel b. Note that $\mathrm{Re}[\chi^{(2)}_S(\omega)]$ and $\mathrm{Im}[\chi^{(2)}_S(\omega)]$ are related by the Kramers−Kronig relation.

In our measurement, the crystalline quartz surface had undergone several cycles of low and high pH values in water for days before the actual spectra were taken. Surface reactions could have made the quartz surface more like a fused silica surface, which was manifested in a gradual change of the peak shape. Figure 14 shows the spectra of

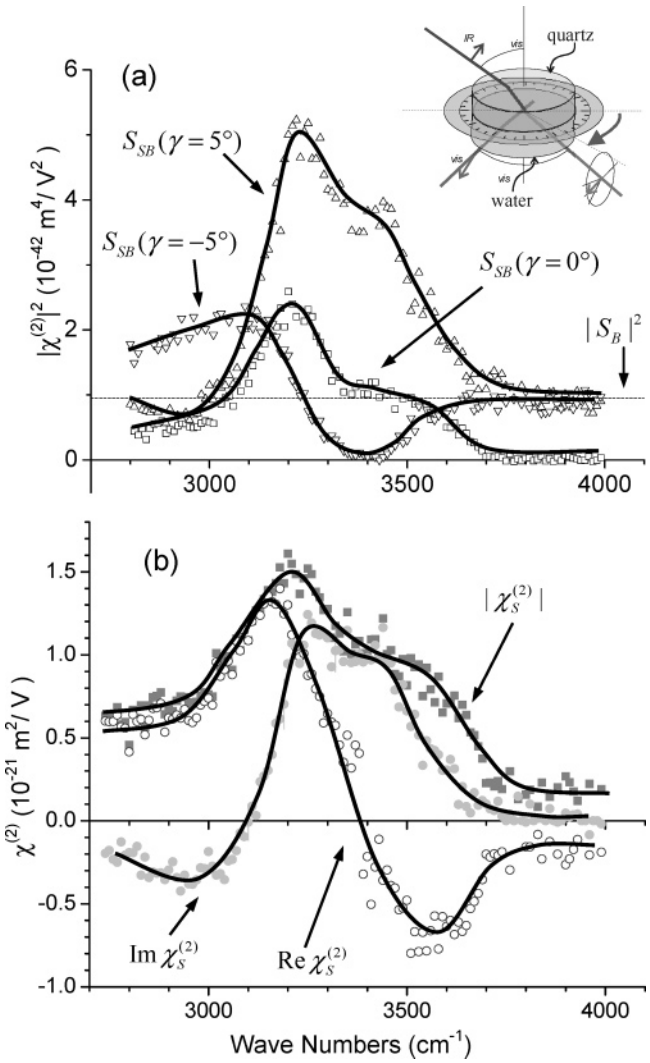

Figure 13. An example of phase-sensitive SFG spectroscopic measurement for a quartz/water interface at pH = 6.5: (a) measured spectra of $S_\gamma(\gamma{=}+5°)$, $S_\gamma(\gamma{=}-5°)$, $S_\gamma(\gamma{=}0°)$, and $|\chi^{(2)}_B/\Delta k|^2$; (b) deduced spectra of $|\chi^{(2)}_S|^2$, $\mathrm{Re}(\chi^{(2)}_S)$, and $\mathrm{Im}(\chi^{(2)}_S)$. The inset shows the experimental arrangement. The azimuthal angle ϕ of the quartz crystal is adjusted to suppress SFG in the SSP polarization combination. The analyzer of the SF output is set either for precise S polarization or at $\pm\gamma$ angle away from S-polarization. Adapted figure with permission from ref 30. Copyright 2005 by the American Physical Society. http://link.aps.org/abstract/PRL/v94/e046102.

$|\chi^{(2)}_S(\omega)|$, $\mathrm{Re}[\chi^{(2)}_S(\omega)]$, and $\mathrm{Im}[\chi^{(2)}_S(\omega)]$ at several different bulk pH values. The spectra of $|\chi^{(2)}_S(\omega)|$ indeed resemble those of water/fused silica interfaces; they all exhibit the icelike and liquidlike peaks. But $\mathrm{Re}[\chi^{(2)}_S(\omega)]$ and $\mathrm{Im}[\chi^{(2)}_S(\omega)]$ appear more complex and vary in both amplitude and sign.

We now focus on $\mathrm{Im}[\chi^{(2)}_S(\omega)]$ because it is more informative. Figure 15 displays a set of $\mathrm{Im}[\chi^{(2)}_S(\omega)]$ obtained with successively decreasing pH. We have found that all spectra of $\mathrm{Im}[\chi^{(2)}_S(\omega)]$ can be decomposed into a liquidlike peak at 3400 cm^{-1} with a profile and line width chosen to be the same as the IR absorption spectrum of bulk water, and an icelike peak composed of two peaks, one at 3200 cm^{-1} with a line width (fwhm) of 170 cm^{-1} and the other at 3000 cm^{-1} with a line width of 250 cm^{-1}. This is seen in Figure 14. The amplitude variations of the three peaks with pH are plotted in Figure 16. It shows that they respond to the increasing pH differently. The liquidlike peak is always

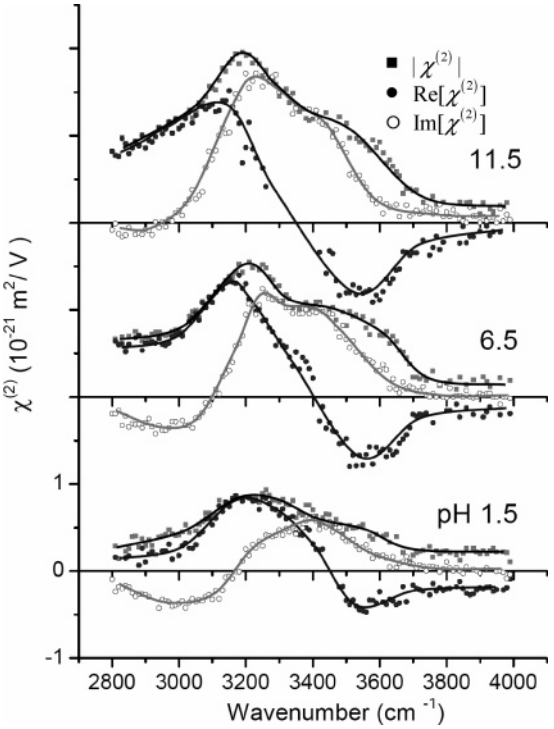

Figure 14. Spectra of $|\chi_S^{(2)}|^2$, Re($\chi_S^{(2)}$), and Im($\chi_S^{(2)}$) for water/α-quartz interface at several pH values of water. Reprinted figure with permission from ref 30. Copyright 2005 by the American Physical Society. http://link.aps.org/abstract/PRL/v94/e046102.

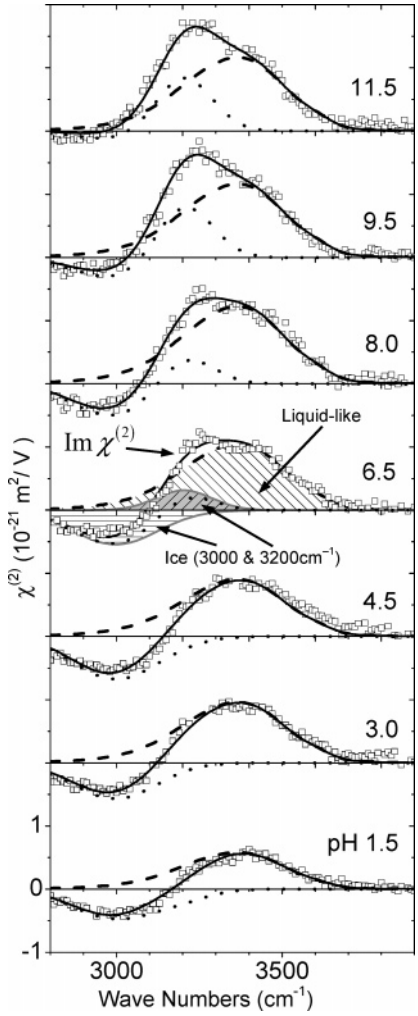

Figure 15. A series of Im[$\chi^{(2)}$] spectra of the water/α-quartz interface at different values of pH. In each spectrum, the solid curve is a fit to the data that comprises a liquidlike peak (dashed curve) and an icelike peak (dotted curves). The liquidlike peak profile is borrowed from the linear absorption spectrum of bulk water, and the icelike component is further decomposed into two subpeaks: a negative and a positive subpeak centered at ~3000 and 3200 cm^{-1} and having fwhm of 250 and 170 cm^{-1}, respectively. The graph for pH = 6.5 explicitly shows the two icelike components (hatched peaks) obtained in the decomposition. Adapted figure with permission from ref 30. Copyright 2005 by the American Physical Society. http://link.aps.org/abstract/PRL/v94/e046102.

positive but increases in strength with increasing pH in the range between 1.5 and 5, indicating that the interfacial water species participating in the more disordered part of the bonding network has an increasing net polar orientation with the H end facing the quartz surface. The change saturates around pH ≈ 7. The two components of the icelike peak vary appreciably with increase of pH from 4 to 10. The lower-frequency component is always negative, but its strength decreases with increase of pH. The higher-frequency component starts essentially with zero strength and becomes increasingly positive after pH ≈ 4 The increase of strengths of the liquidlike peak and the high-frequency component of the icelike peak with pH can be understood by increase of the net polar orientation with H facing the surface, knowing that the quartz surface should be increasingly negatively charged with increase of pH and the resulting surface field should reorient water molecules with H facing the surface. The lower-frequency component at 3000 cm^{-1} is a feature also seen in the spectra of ice/vapor and ice/silica interfaces either as a small peak or as a small shoulder of the main peak.[120,121] It comes from the OH of water species in the icelike ordered structure with a net polarization of O facing the surface.

The PS-SFVS results provide us with more detailed information about the water interfacial structure at the quartz/water interfaces. Immersed in water, the quartz surface is obviously not homogeneous. It appears to have two different binding sites for water molecules. Those contributing to the liquidlike peak and participating in a hydrogen-bonding structure very much like that of bulk water are associated with binding sites that are more easily deprotonated. They have a net polar orientation with H pointing toward the surface. As pH increases, more of these surface sites are deprotonated, and more water molecules appear to be reoriented with H toward the surface presumably by the negative charges at the deprotonated sites. Saturation of the strength of the liquidlike peak indicates that these surface sites are almost fully deprotonated at pH ≈ 7. Water molecules contributing to the icelike peak (assuming both components originate from water molecules) are associated with surface binding sites that are less easily deprotonated. Below pH ≈ 4, there is a net polar orientation of OH bonds with O facing the surface. Deprotonation of these surface sites appears to set in at pH ≈ 4. With further increase of pH, the increasing number of negatively charged surface sites poles the associated water molecules with H toward the surface. Saturation of deprotonation, and hence reorientation of water molecules, at these sites occur at pH ≈ 10−11.

Eisenthal and co-workers,[122] based on their SHG measurement, first proposed the presence of two different surface sites for water adsorption on silica. Their result is reproduced in Figure 17. It is seen that the SH output field versus pH has two plateaus, one at pH ≈ 6 and the other at pH ≈ 12.

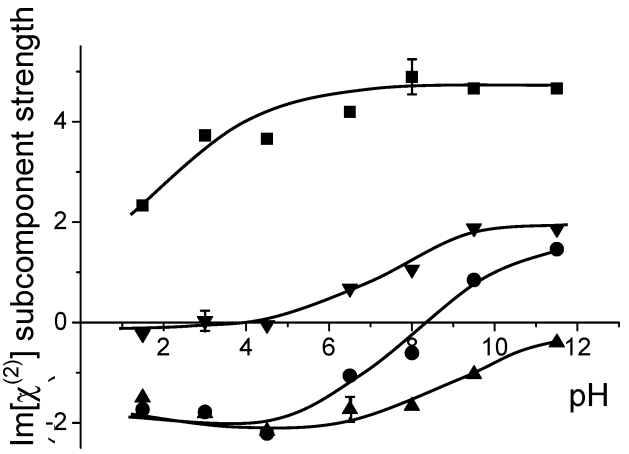

Figure 16. Strengths of various components obtained from decomposition of the spectra in Figure 15 as functions of pH: (■) liquidlike peak; (▲) 3000 cm^{-1} icelike component; (▼) 3200 cm^{-1} icelike component; (●) combined strength of the two icelike components. Reprinted figure with permission from ref 30. Copyright 2005 by the American Physical Society. http://link.aps.org/abstract/PRL/v94/e046102.

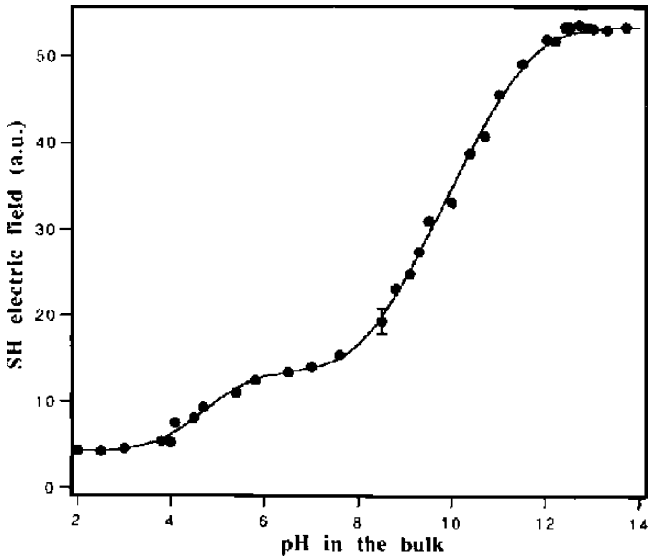

Figure 17. Second harmonic output field from a water/fused silica interface as a function of pH. Reprinted from ref 122, Copyright 1992, with permission from Elsevier.

They interpreted the result as arising from water molecules binding to two different surface sites with different p*K* values for deprotonation. Our SFVS result supports their conclusion. The quantitative difference in pH variation could be due to preparation of the silica surface.

6. Discussion

SFVS has been very successful in providing vibrational spectra for water interfaces much needed for understanding of interfacial water structure. However, without theoretical guidance, interpretation of the spectra is not an easy matter. A surface water spectrum obtained by the conventional SFVS in the OH stretch region is usually comprised of an icelike peak at ~3200 cm^{-1} and a liquidlike peak at ~3400 cm^{-1}. An additional dangling OH peak may appear at ~3700 cm^{-1} if the opposite medium is hydrophobic. The broad icelike and liquidlike peaks are enhanced if the interface is charged by protonation, deprotonation, or ion adsorption, although the relative enhancement may be different. This is a description generally accepted by all workers in the field. Beyond this, in connection with the interfacial water structure, the interpretation becomes more speculative and varies among researchers. There are two main difficulties in analyzing and interpreting the spectrum. First, the SF response comes from an orientational distribution with a net polar orientational order but not from a distribution with only a nonpolar orientational order of water molecules. This was often forgotten or ignored in the interpretation. Thus enhancement of the icelike or liquidlike peak does not necessarily mean an increasing number of water molecules contributing to the peak. It only means that there are more polar-oriented molecules. Because the SF output is proportional to $|\chi_S^{(2)}(\omega)|^2$, the direction of polar orientation is not known. Second, decomposition of the SF $|\chi_S^{(2)}(\omega)|^2$ spectrum of water can hardly be unique, especially if the relative signs of the components are not known. This could lead to erroneous interpretation of the spectrum and incorrect description of the interfacial structure. For example, Richmond and co-workers fitted their water/vapor spectra first with the amplitudes, A_q, of the free OH mode and the liquidlike mode having the same sign[66] and, more recently, with opposite signs.[67−69] The two cases correspond to very different OH orientations: one has the liquidlike bonded OH having a net polar orientation the same as that of the dangling OH and the other opposite. The PS-SFVS measurement shows that free OH and bonded OH for the liquidlike peak have the same net polar orientation.

The spectrum obtained by PS-SFVS is an improvement but does not solve all the problems. It yields separately the spectra of $\mathrm{Re}[\chi_S^{(2)}(\omega)]$ and $\mathrm{Im}[\chi_S^{(2)}(\omega)]$. They can be positive or negative. The sign of $\mathrm{Im}[\chi_S^{(2)}(\omega)]$ describes the direction of the net polar orientation of the molecules, which can now be determined without relying on fitting of the spectrum. However, it is still proportional to the surface density of net polar-oriented molecules and its decomposition into resonant peaks, although improved, still has some uncertainty. In the case of silica/water interfaces, we could fit each spectrum of $\mathrm{Im}[\chi_S^{(2)}(\omega)]$ by assuming it is composed of a liquidlike peak and an icelike portion. As seen in Figure 15, the fit is good for all spectra even if we impose the strict conditions that the liquidlike peak has the same profile as the infrared spectrum of the bulk water and the two components of the icelike peak have fixed resonant frequencies and line widths. The profile of the liquidlike peak assumed here is quite different from those deduced from fitting the spectrum of $|\chi_S^{(2)}(\omega)|$ but is more reasonable considering that the disordered hydrogen bonding of water molecules at the surface and in the bulk should not be very different. An immediate consequence of the broader liquidlike peak is that the icelike peak is correspondingly much weaker. The two components of the icelike peak in $\mathrm{Im}[\chi_S^{(2)}(\omega)]$ have different signs at low pH, indicating that they must come from two different OH species with opposite net polar orientations. This is also not obvious from the spectrum of $|\chi_S^{(2)}(\omega)|$. The pH dependence of the peaks allows us to identify the existence of two different surface adsorption sites.

To understand the results of Figures 15 and 16 and answer the question why molecules responsible for the liquidlike peak always have a net polar orientation with H pointing toward the surface and molecules for the lower-frequency and higher-frequency components of the icelike peak have net polar orientations with O and H pointing toward the

surface, respectively, we need theoretical guidance. In its absence, we have to resort to a reasonable physical model. Reference 30 used a simple picture that water molecules would hydrogen bond with O to H at hydrogen-terminated surface sites and H to O at deprotonated sites on quartz. At very low pH, all the surface sites on silica are supposed to be fully protonated. Then the observation that molecules in the liquidlike peak still had a net polarization with H facing the surface could only be explained by assuming the existence of residual surface sites that remain deprotonated even at very low pH. On the other hand, molecules in the low-frequency component of the icelike peak have always a net polar orientation with O facing the surface even at very high pH. This could only be explained by assuming the existence of residual surface sites that remain always protonated. The above picture is not very satisfactory. Here we present a more plausible model proposed by Lee and Rossky based on their molecular dynamics simulation.[35]

We consider that the interfacial water structure more or less resembles a (disordered) tetrahedral hydrogen-bonding network of hexagonal ice. At each H-terminated silica site, the oxygen of SiOH can have two water molecules hydrogen-bonded to it. (A third water molecule can hydrogen-bond with O to H of SiOH; see Figure 9a). If the site is deprotonated, three water molecules can be hydrogen-bonded with H to the oxygen (Figure 9b). Then, it can be shown that for interfacial water with a more or less icelike structure, there are always more OH bonds with H facing the surface, and the excess number increases with increasing number of deprotonated surface sites. This explains why molecules in the liquidlike peak and the high-frequency component of the icelike peak always have a net polar orientation with H facing the surface. It also explains why the two grow with increase of pH. The low-frequency component at 3000 cm^{-1} could be assigned to the OH stretch of SiOH at the protonated sites.[123] However since it is always seen in the spectrum of ice interfaces,[120,121] we suspect that it is an integral part of the icelike spectral peak. As in the ice case, the icelike peak would be interpreted as originating from coupled OH (phonon) modes of the ordered bonding network. The higher-frequency component would then have more participation of OH with H pointing toward the surface and the lower-frequency component more participation of OH with O pointing toward the surface. If this picture is correct, we should expect to see a similar icelike peak in the spectrum of $\mathrm{Im}[\chi_S^{(2)}(\omega)]$ for other water interfaces. Hopefully, molecular dynamics simulations could also reproduce such an icelike spectral peak.

The above case of quartz/water interface illustrates how PS-SFVS can help analyze and understand the surface vibrational spectrum of water and yield more detailed information about the water interfacial structure. As in all spectroscopic studies, however, the true detailed understanding often has to come out of comparison of theory with experiment. For water interfaces, all SF vibrational spectra of $|\chi_S^{(2)}(\omega)|^2$ seem to possess the same characteristic icelike and liquidlike features. The PS-SFVS spectra probably could reveal more differences in spectra of different interfaces. It is particularly important to obtain the PS-SF spectra for vapor/water and vapor/ice interfaces because they can serve as references for the other water interfaces. However, the PS-SFG technique described in this paper is only applicable to interfaces where the substrate can provide a suitable $\chi_B^{(2)}$ to interfere with $\chi_S^{(2)}$. We are in the process of developing a more general interference method that would allow PS-SFG studies of all accessible interfaces.

7. Conclusion

SFVS is powerful as the only technique that provides vibrational spectra for water interfaces. It has been used extensively to probe structures of water interfaces of all kinds. The spectrum of the SSP input/output polarization combinations usually shows an icelike peak at ~3200 cm^{-1} and a liquidlike peak at ~3400 cm^{-1}, plus a narrow dangling OH peak at ~3700 cm^{-1} if the interface is hydrophobic. The icelike and liquidlike peaks suggest that the interfacial water molecules form a partially ordered and partially disordered hydrogen-bonding network. Protonation, deprotonation, and ion and molecular adsorption at a water interface may significantly change the spectrum. A surface field, created by surface charges, for example, tends to enhance the spectrum.

Detailed interpretations of surface water spectra, however, are often misleading because of two difficulties in analyzing a spectrum. First, the SF spectral peak in terms of resonance in the nonlinear susceptibility, $|\chi_S^{(2)}(\omega)|$, is proportional not to the total number of contributing molecules, but to the number of net polar-oriented molecules. Thus an increased strength of the icelike peak does not necessarily mean that there are more molecules participating in the more ordered regions of the network, but only indicates that the total number of polar-oriented molecules in the more ordered regions has increased. A surface field can induce more polar-oriented molecules in a spectral peak but does not necessarily increase the total number of molecules contributing to the peak. (More specifically, the observed enhancement of the icelike peak induced by a surface field does not necessarily mean that the interfacial water network is more ordered unless there is complementary evidence.) Second, decomposition of a spectrum of overlapping peaks is often not unique. Too much confidence in the decomposition could lead to incorrect description of the interfacial water structure. Molecular dynamics simulations can help, but unfortunately, they also have limitations.

PS-SFVS yields $\mathrm{Re}[\chi_S^{(2)}(\omega)]$ and $\mathrm{Im}[\chi_S^{(2)}(\omega)]$ and allows determination of the net polar-orienting directions of molecules that contribute to the various peaks. Because the signs of $\mathrm{Re}[\chi_S^{(2)}(\omega)]$ and $\mathrm{Im}[\chi_S^{(2)}(\omega)]$ are now known, decomposition of a spectrum into overlapping peaks becomes more reliable. Work on water/quartz interfaces with different pH has generated interesting results. The spectrum of $\mathrm{Im}[\chi_S^{(2)}(\omega)]$ can be decomposed into a liquidlike peak at ~3400 cm^{-1} with a profile the same as that of the infrared absorption spectrum of bulk water and an icelike peak composed of a main component at ~3200 cm^{-1} with a line width (fwhm) of 170 cm^{-1} and a weaker component at ~3000 cm^{-1} with a line width of 250 cm^{-1}. The pH dependences of the two peaks are very different, suggesting that there are two different surface sites for water molecules to adsorb. Molecules in the liquidlike peak adsorb at more easily deprotonated sites. They adsorb with a net polar orientation of H facing the surface. Molecules involved in the higher-frequency component of the icelike peak also have a net polar orientation of H facing the surface, but those in the low-frequency component have the opposite net polar orientation. Since both components are also observed in the spectra of real ice interfaces, we have to consider them as

integral parts of an icelike peak resulting from coupled OH modes of molecules in an ordered network. The weaker component disappears when the adsorption sites are fully deprotonated.

The new picture presented above for water/quartz interfaces is still speculative and needs to be confirmed by molecular dynamics simulations. We expect that the interfacial structure of water at other interfaces is qualitatively similar as long as interactions of water molecules with the substrate do not dominate over interactions between water molecules with detailed differences appearing in the net polar orientations of molecules in the icelike and liquidlike regions. Thus it is important to obtain PS-SFVS spectra for other water interfaces. Through correlation of these spectra, we should be able to paint a more correct picture for the interfacial water structure and its variation with the substrate and environment. The neat vapor/water and vapor/ice interfaces could act as the reference surfaces.

8. Acknowledgment

This work was supported by the STC program of the National Science Foundation under Agreement Number CTS-0120978 and partially supported by the U.S. Department of Energy under Contract No. DE-AC03-76SF00098.

9. References

(1) Ball, P. *Nature* **2003**, *423*, 25.
(2) Israelachvili, J.; Wennerstrom, H. *Nature* **1996**, *379*, 219.
(3) *Water. A Comprehensive Treatise*; Franks, F., Ed.; Plenum Press: New York, 1979; Vol. 1−6.
(4) Mitsui, T.; Rose, M. K.; Fomin, E.; Ogletree, D. F.; Salmeron, M. *Science* **2002**, *297*, 1850.
(5) Cerda, J.; Michaelides, A.; Bocquet, M. L.; Feibelman, P. J.; Mitsui, T.; Rose, M.; Fomin, E.; Salmeron, M. *Phys. Rev. Lett.* **2004**, *93*, No. 116101.
(6) *Nano-Surface Chemistry*; Rosoff, M., Ed.; Marcel Dekker: New York, 2002.
(7) Tyrrell, J. W. G.; Attard, P. *Phys. Rev. Lett.* **2001**, *8717*, No. 176104.
(8) Ghosal, S.; Hemminger, J. C.; Bluhm, H.; Mun, B. S.; Hebenstreit, E. L. D.; Ketteler, G.; Ogletree, D. F.; Requejo, F. G.; Salmeron, M. *Science* **2005**, *307*, 563.
(9) Pershan, P. S. *Physica A* **1993**, *200*, 50.
(10) Toney, M. F.; Howard, J. N.; Richer, J.; Borges, G. L.; Gordon, J. G.; Melroy, O. R.; Wiesler, D. G.; Yee, D.; Sorensen, L. B. *Nature* **1994**, *368*, 444.
(11) Wilson, K. R.; Rude, B. S.; Catalano, T.; Schaller, R. D.; Tobin, J. G.; Co, D. T.; Saykally, R. J. *J. Phys. Chem. B* **2001**, *105*, 3346.
(12) Wilson, K. R.; Schaller, R. D.; Co, D. T.; Saykally, R. J.; Rude, B. S.; Catalano, T.; Bozek, J. D. *J. Chem. Phys.* **2002**, *117*, 7738.
(13) Wilson, K. R.; Rude, B. S.; Smith, J.; Cappa, C.; Co, D. T.; Schaller, R. D.; Larsson, M.; Catalano, T.; Saykally, R. J. *Rev. Sci. Instrum.* **2004**, *75*, 725.
(14) Reedijk, M. F.; Arsic, J.; Hollander, F. F. A.; de Vries, S. A.; Vlieg, E. *Phys. Rev. Lett.* **2003**, *90*, No. 066103.
(15) Jensen, T. R.; Jensen, M. O.; Reitzel, N.; Balashev, K.; Peters, G. H.; Kjaer, K.; Bjornholm, T. *Phys. Rev. Lett.* **2003**, *90*, No. 086101.
(16) Steitz, R.; Gutberlet, T.; Hauss, T.; Klosgen, B.; Krastev, R.; Schemmel, S.; Simonsen, A. C.; Findenegg, G. H. *Langmuir* **2003**, *19*, 2409.
(17) Schwendel, D.; Hayashi, T.; Dahint, R.; Pertsin, A.; Grunze, M.; Steitz, R.; Schreiber, F. *Langmuir* **2003**, *19*, 2284.
(18) Shen, Y. R. *Nature* **1989**, *337*, 519.
(19) Shen, Y. R. In *Frontier in Laser Spectroscopy*; Hansch, T. W., Inguscio, M., Eds.; North-Holland: Amsterdam, 1994.
(20) Miranda, P. B.; Shen, Y. R. *J. Phys. Chem. B* **1999**, *103*, 3292.
(21) Eisenthal, K. B. *Chem. Rev.* **1996**, *96*, 1343.
(22) Richmond, G. L. *Chem. Rev.* **2002**, *102*, 2693.
(23) Du, Q.; Superfine, R.; Freysz, E.; Shen, Y. R. *Phys. Rev. Lett.* **1993**, *70*, 2313.
(24) Du, Q.; Freysz, E.; Shen, Y. R. *Science* **1994**, *264*, 826.
(25) Du, Q.; Freysz, E.; Shen, Y. R. *Phys. Rev. Lett.* **1994**, *72*, 238.
(26) Shultz, M. J.; Baldelli, S.; Schnitzer, C.; Simonelli, D. *J. Phys. Chem. B* **2002**, *106*, 5313.
(27) Liu, D. F.; Ma, G.; Levering, L. M.; Allen, H. C. *J. Phys. Chem. B* **2004**, *108*, 2252.
(28) Kim, G.; Gurau, M.; Kim, J.; Cremer, P. S. *Langmuir* **2002**, *18*, 2807.
(29) Nihonyanagi, S.; Shen, Y.; Uosaki, K.; Dreesen, L.; Humbert, C.; Thiry, P.; Peremans, A. *Surf. Sci.* **2004**, *573*, 11.
(30) Ostroverkhov, V.; Waychunas, G. A.; Shen, Y. R. *Phys. Rev. Lett.* **2005**, *94*, No. 046102.
(31) Frenkel, J. *Kinetic Theory of Liquids*; Dover: New York, 1955.
(32) *Chemistry and Physics of Interfaces I*; Ross, S., Ed.; American Physical Society Publications: Washington, DC, 1965.
(33) Lee, C. Y.; McCammon, J. A.; Rossky, P. J. *J. Chem. Phys.* **1984**, *80*, 4448.
(34) Rossky, P. J.; Lee, S. H. *Chem. Scr.* **1989**, *29A*, 93.
(35) Lee, S. H.; Rossky, P. J. *J. Chem. Phys.* **1994**, *100*, 3334.
(36) Benjamin, I. *Phys. Rev. Lett.* **1994**, *73*, 2083.
(37) Knipping, E. M.; Lakin, M. J.; Foster, K. L.; Jungwirth, P.; Tobias, D. J.; Gerber, R. B.; Dabdub, D.; Finlayson-Pitts, B. J. *Science* **2000**, *288*, 301.
(38) Morita, A.; Hynes, J. T. *Chem. Phys.* **2000**, *258*, 371.
(39) Morita, A.; Hynes, J. T. *J. Phys. Chem. B* **2002**, *106*, 673.
(40) Jungwirth, P.; Tobias, D. J. *J. Phys. Chem. B* **2000**, *104*, 7702.
(41) Jungwirth, P.; Tobias, D. J. *J. Phys. Chem. B* **2001**, *105*, 10468.
(42) Jungwirth, P.; Tobias, D. J. *J. Phys. Chem. B* **2002**, *106*, 6361.
(43) Jedlovszky, P. *J. Phys.: Condens. Matter* **2004**, *16*, S5389.
(44) Jedlovszky, P.; Vincze, A.; Horvai, G. *Phys. Chem. Chem. Phys.* **2004**, *6*, 1874.
(45) Perry, A.; Ahlborn, H.; Space, B.; Moore, P. B. *J. Chem. Phys.* **2003**, *118*, 8411.
(46) Feibelman, P. J. *Chem. Phys. Lett.* **2004**, *389*, 92.
(47) Puibasset, J.; Pellenq, R. J. M. *J. Chem. Phys.* **2003**, *119*, 9226.
(48) Puibasset, J.; Pellenq, R. J. M. *Phys. Chem. Chem. Phys.* **2004**, *6*, 1933.
(49) Marx, D. *Science* **2004**, *303*, 634.
(50) Kuo, I. F. W.; Mundy, C. J. *Science* **2004**, *303*, 658.
(51) Benjamin, I. *J. Chem. Phys.* **2004**, *121*, 10223.
(52) Garrett, B. C. *Science* **2004**, *303*, 1146.
(53) Morita, A. *Chem. Phys. Lett.* **2004**, *398*, 361.
(54) Brown, M. G.; Walker, D. S.; Raymond, E. A.; Richmond, G. L. *J. Phys. Chem. B* **2003**, *107*, 237.
(55) Buch, V. *J. Phys. Chem. B* **2005**, *109*, 17771.
(56) Perry, A.; Neipert, C.; Kasprzyk, C. R.; Green, T.; Space, B.; Moore, P. B. *J. Chem. Phys.* **2005**, *123*, No. 144705.
(57) Perry, A.; Neipert, C.; Ridley, C.; Space, B.; Moore, P. B. *Phys Rev E* **2005**, *71*, No. 050601.
(58) Oudar, J. L.; Shen, Y. R. *Phys. Rev. A* **1980**, *22*, 1141.
(59) Bertie, J. E.; Labbe, H. J.; Whally, E. *J. Chem. Phys.* **1969**, *50*, 4501.
(60) Querry, M. R.; Wieliczka, D. M.; Segelstein, D. J. In *Handbook of Optical Constants of Solids II*; Academic Press: Boston, MA, 1991.
(61) Kipling, J. J. *J. Colloid Sci.* **1963**, *18*, 502.
(62) Wei, X.; Shen, Y. R. *Phys. Rev. Lett.* **2001**, *86*, 4799.
(63) Gragson, D. E.; McCarty, B. M.; Richmond, G. L. *J. Phys. Chem.* **1996**, *100*, 14272.
(64) Gragson, D. E.; McCarty, B. M.; Richmond, G. L. *J. Am. Chem. Soc.* **1997**, *119*, 6144.
(65) Gragson, D. E.; Richmond, G. L. *J. Phys. Chem. B* **1998**, *102*, 3847.
(66) Brown, M. G.; Raymond, E. A.; Allen, H. C.; Scatena, L. F.; Richmond, G. L. *J. Phys. Chem. A* **2000**, *104*, 10220.
(67) Raymond, E. A.; Tarbuck, T. L.; Richmond, G. L. *J. Phys. Chem. B* **2002**, *106*, 2817.
(68) Raymond, E. A.; Tarbuck, T. L.; Brown, M. G.; Richmond, G. L. *J. Phys. Chem. B* **2003**, *107*, 546.
(69) Raymond, E. A.; Richmond, G. L. *J. Phys. Chem. B* **2004**, *108*, 5051.
(70) Baldelli, S.; Schnitzer, C.; Shultz, M. J.; Campbell, D. J. *J. Phys. Chem. B* **1997**, *101*, 10435.
(71) Baldelli, S.; Schnitzer, C.; Shultz, M. J.; Campbell, D. J. *J. Phys. Chem. B* **1997**, *101*, 4607.
(72) Baldelli, S.; Schnitzer, C.; Shultz, M. J.; Campbell, D. J. *Chem. Phys. Lett.* **1998**, *287*, 143.
(73) Baldelli, S.; Schnitzer, C.; Campbell, D. J.; Shultz, M. J. *J. Phys. Chem. B* **1999**, *103*, 2789.
(74) Baldelli, S.; Schnitzer, C.; Shultz, M. J. *Chem. Phys. Lett.* **1999**, *302*, 157.
(75) Schnitzer, C.; Baldelli, S.; Campbell, D. J.; Shultz, M. J. *J. Phys. Chem. A* **1999**, *103*, 6383.
(76) Schnitzer, C.; Baldelli, S.; Shultz, M. J. *J. Phys. Chem. B* **2000**, *104*, 585.
(77) Shultz, M. J.; Schnitzer, C.; Simonelli, D.; Baldelli, S. *Int. Rev. Phys. Chem.* **2000**, *19*, 123.
(78) Simonelli, D.; Shultz, M. J. *J. Chem. Phys.* **2000**, *112*, 6804.
(79) Simonelli, D.; Shultz, M. J. *J. Mol. Spectrosc.* **2001**, *205*, 221.
(80) Mucha, M.; Frigato, T.; Levering, L. M.; Allen, H. C.; Tobias, D. J.; Dang, L. X.; Jungwirth, P. *J. Phys. Chem. B* **2005**, *109*, 7617.

(81) Allen, H. C.; Raymond, E. A.; Richmond, G. L. *Curr. Opin. Colloid Interface Sci.* **2000**, *5*, 74.
(82) Allen, H. C.; Raymond, E. A.; Richmond, G. L. *J. Phys. Chem. A* **2001**, *105*, 1649.
(83) Wilson, K. R.; Cavalleri, M.; Rude, B. S.; Schaller, R. D.; Nilsson, A.; Pettersson, L. G. M.; Goldman, N.; Catalano, T.; Bozek, J. D.; Saykally, R. J. *J. Phys.: Condens. Matter* **2002**, *14*, L221.
(84) Miranda, P. B.; Du, Q.; Shen, Y. R. *Chem. Phys. Lett.* **1998**, *286*, 1.
(85) Gavish, M.; Popovitzbiro, R.; Lahav, M.; Leiserowitz, L. *Science* **1990**, *250*, 973.
(86) Patey, G. N.; Torrie, G. M. *Chem. Scr.* **1989**, *29A*, 39.
(87) Raduge, C.; Pflumio, V.; Shen, Y. R. *Chem. Phys. Lett.* **1997**, *274*, 140.
(88) Schnitzer, C.; Baldelli, S.; Shultz, M. J. *Chem. Phys. Lett.* **1999**, *313*, 416.
(89) Baldelli, S.; Schnitzer, C.; Shultz, M. J. *J. Chem. Phys.* **1998**, *108*, 9817.
(90) Johnson, C. M.; Tyrode, E.; Baldelli, S.; Rutland, M. W.; Leygraf, C. *J. Phys. Chem. B* **2005**, *109*, 321.
(91) Petersen, P. B.; Johnson, J. C.; Knutsen, K. P.; Saykally, R. J. *Chem. Phys. Lett.* **2004**, *397*, 46.
(92) Petersen, P. B.; Saykally, R. J. *Chem. Phys. Lett.* **2004**, *397*, 51.
(93) Petersen, P. B.; Saykally, R. J. *J. Phys. Chem. B* **2005**, *109*, 7976.
(94) Dang, L. X. *J. Chem. Phys.* **2003**, *119*, 6351.
(95) Petersen, M. K.; Iyengar, S. S.; Day, T. J. F.; Voth, G. A. *J. Phys. Chem. B* **2004**, *108*, 14804.
(96) Nihonyanagi, S.; Ye, S.; Uosaki, K. *Electrochim. Acta* **2001**, *46*, 3057.
(97) Kim, J.; Kim, G.; Cremer, P. S. *J. Am. Chem. Soc.* **2002**, *124*, 8751.
(98) Gurau, M. C.; Kim, G.; Lim, S. M.; Albertorio, F.; Fleisher, H. C.; Cremer, P. S. *ChemPhysChem* **2003**, *4*, 1231.
(99) Li, I.; Bandara, J.; Shultz, M. J. *Langmuir* **2004**, *20*, 10474.
(100) Ostroverkhov, V.; Waychunas, G. A.; Shen, Y. R. *Chem. Phys. Lett.* **2004**, *386*, 144.
(101) Iler, R. K. *The Chemistry of Silica*; John Wiley & Sons: New York, 1979.
(102) Yeganeh, M. S.; Dougal, S. M.; Pink, H. S. *Phys. Rev. Lett.* **1999**, *83*, 1179.
(103) Becraft, K. A.; Richmond, G. L. *Langmuir* **2001**, *17*, 7721.
(104) Becraft, K. A.; Moore, F. G.; Richmond, G. L. *Phys. Chem. Chem. Phys.* **2004**, *6*, 1880.
(105) Becraft, K. A.; Moore, F. G.; Richmond, G. L. *J. Phys. Chem. B* **2003**, *107*, 3675.
(106) Kataoka, S.; Gurau, M. C.; Albertorio, F.; Holden, M. A.; Lim, S. M.; Yang, R. D.; Cremer, P. S. *Langmuir* **2004**, *20*, 1662.
(107) Chu, Y. S.; Lister, T. E.; Cullen, W. G.; You, H.; Nagy, Z. *Phys. Rev. Lett.* **2001**, *86*, 3364.
(108) Ruan, C. Y.; Lobastov, V. A.; Vigliotti, F.; Chen, S. Y.; Zewail, A. H. *Science* **2004**, *304*, 80.
(109) Carnie, S. L.; Torrie, G. M. *Adv. Chem. Phys.* **1984**, *56*, 141.
(110) Scatena, L. F.; Richmond, G. L. *J. Phys. Chem. B* **2001**, *105*, 11240.
(111) Scatena, L. F.; Brown, M. G.; Richmond, G. L. *Science* **2001**, *292*, 908.
(112) Scatena, L. F.; Richmond, G. L. *Chem. Phys. Lett.* **2004**, *383*, 491.
(113) Scatena, L. F.; Richmond, G. L. *J. Phys. Chem. B* **2004**, *108*, 12518.
(114) Walker, D. S.; Brown, M.; McFearin, C. L.; Richmond, G. L. *J. Phys. Chem. B* **2004**, *108*, 2111.
(115) Chang, R. K.; Ducuing, J.; Bloembergen, N. *Phys. Rev. Lett.* **1965**, *15*, 6.
(116) Superfine, R.; Huang, J. Y.; Shen, Y. R. *Opt. Lett.* **1990**, *15*, 1276.
(117) Janz, S.; Lu, Z. H. *J. Opt. Soc. Am. B* **1997**, *14*, 1647.
(118) Wilson, P. T.; Jiang, Y.; Carriles, R.; Downer, M. C. *J. Opt. Soc. Am. B* **2003**, *20*, 2548.
(119) Singh, S. In *Handbook of Lasers*; Pressley, R. J., Ed.; Chemical Rubber Co.: Cleveland, OH, 1971.
(120) Wei, X.; Miranda, P. B.; Shen, Y. R. *Phys. Rev. Lett.* **2001**, *86*, 1554.
(121) Wei, X.; Miranda, P. B.; Zhang, C.; Shen, Y. R. *Phys. Rev. B* **2002**, *66*, No. 085401.
(122) Ong, S. W.; Zhao, X. L.; Eisenthal, K. B. *Chem. Phys. Lett.* **1992**, *191*, 327.
(123) This mode would have the same pH dependence as the high-frequency icelike peak because they are associated with the same adsorption sites. We thank Dr. H. Morita for confirming this possible assignment.

CR040377D